RHO-LIKE MESONS FROM ANALYSIS OF THE PION-PION SCATTERING

Yu.S. Surovtsev[a] and P. Bydžovský[b]

(a) *Bogoliubov Laboratory of Theoretical Physics, JINR, Dubna 141 980, Russia*
(b) *Nuclear Physics Institute, ASCR, 25068 Řež, Czech Republic*

Abstract

Considering analyticity, unitarity and an influence of coupled channels, experimental data on the isovector P-wave of $\pi\pi$ scattering was analyzed to study ρ-like mesons below 1900 MeV. The analysis indicates evidently that in the energy range 1200–1800 MeV, there are three ρ-like mesons: $\rho(1250)$, $\rho(1450)$ and $\rho(1600)$, unlike the PDG tables. The obtained P-wave $\pi\pi$-scattering length $(a_1^1 = 33.9 \pm 2.02 \; [10^{-3} m_{\pi^+}^{-3}])$ most matches to the one calculated in the local Nambu–Jona-Lasinio model.

1 Introduction

The investigation of vector mesons is actual up to now due to their role in forming the electromagnetic structure of particles and because, *e.g.*, in the ρ-family, only the $\rho(770)$ meson can be deemed to be well understood [1]. The other ρ-like mesons must be either still confirmed in various experiments and analyses or their parameters essentially corrected. For example, the $\rho(1250)$ meson which was discussed actively some time ago [2, 3] was confirmed relatively recently in the amplitude analysis of the LASS Collaboration [4] and in combined analysis of several processes [5]. However this state is referred to only slightly in the PDG issue [1] (the relevant observations are listed under the $\rho(1450)$).

On the other hand, the $\pi\pi$ interaction plays a central role in physics of strongly interacting particles and, therefore, it has always been an object of continuous investigation. Let us note only some recent works devoted also to the theoretical study of the isovector P-wave of $\pi\pi$ scattering. First, there are the analyses of available experimental data on the $\pi\pi$ scattering utilizing the Roy equations [6, 7, 8] and the forward dispersion relations [9, 10], in which, *e.g.*, low-energy parameters of the $\pi\pi$ scattering were obtained. Second, there are the works in which the low-energy parameters are calculated in chiral theories with the linear realization of chiral symmetry [11, 12].

We use our model-independent method [13]. It is based on the first principles (analyticity and unitarity) directly applied to analysis of experimental data. Our aim is to study the ρ-like mesons below 1900 MeV and to obtain the $\pi\pi$-scattering length. Unfortunately this method, using essentially an uniformizing variable, is applicable only to the 2-channel case and under some conditions to the 3-channel one. Here the thresholds of the $\pi\pi$ and $\omega\pi$ channels are allowed for explicitly in the uniformizing variable (in the threshold region of the second channel, one has observed a deviation from elasticity of the P-wave $\pi\pi$ scattering). Influence of other coupled channels is supposed to be taken into account through the background. In order to investigate a

coupling of resonances with these other channels, we also apply multichannel Breit–Wigner forms to generate the resonance poles.

The paper is organized as follows. In Section II, we outline the method of the uniformizing variable in applying it to studying the 2-channel $\pi\pi$ scattering and present results of the analysis of the available data [14]–[16] on the isovector P-wave of $\pi\pi$ scattering. Section III is devoted to analysis of the same data using the Breit–Wigner forms. Finally, in Section VI, we summarize and discuss obtained results.

2   Analysis of P-wave $\pi\pi$ scattering in the uniformizing variable method

Let the $\pi\pi$-scattering S-matrix be determined on the 4-sheeted Riemann surface with the right-hand branch-points at $4m_{\pi^+}^2$ and $(m_\omega + m_{\pi^0})^2$ and also with the left-hand one at $s = 0$. It is supposed that influence of other branch points can be taken into account through the background. The Riemann-surface sheets are numbered according to the signs of analytic continuations of the channel momenta

$$k_1 = \frac{1}{2}\sqrt{s - 4m_{\pi^+}^2} \quad \text{and} \quad k_2 = \frac{1}{2}\sqrt{s - (m_\omega + m_{\pi^0})^2}$$

as follows: $\text{signs}(\text{Im}k_1, \text{Im}k_2) = ++, -+, --$ and $+-$ correspond to sheets I, II, III and IV, respectively.

The S-matrix is supposed to be $S = S_{res}S_{bg}$ where S_{res} represents resonances and S_{bg}, the background. In general, an explicit allowance for the $(m_\omega + m_{\pi^0})^2$ branch point would permit us to describe transitions between the $\pi\pi$ and $\omega\pi$ initial and final states with the help of the only one function $d(k_1, k_2)$ (the Jost matrix determinant) using the Le Couteur–Newton relations [17]. Unfortunately, the data on process $\pi\pi \to \omega\pi$ are absent.

In Ref. [13] it was shown how one can obtain the multichannel resonance representations by poles and zeros on the Riemann surface with the help of the formulas, expressing analytic continuations of the matrix elements, describing the coupled processes, to unphysical sheets in terms of those on sheet I. It is convenient to start from resonance zeros on sheet I. Then in the 2-channel $\pi\pi$ scattering, we have *three types* of resonances: (**a**) described by a pair of complex conjugate zeros in the S-matrix element on sheet I and by a pair of conjugate shifted zeros on sheet IV; (**b**) described by a pair of conjugate zeros on sheet III and by a pair of conjugate shifted zeros on sheet IV; (**c**) which correspond to a pair of conjugate zeros on sheet I, the one on sheet III and two pairs of conjugate zeros on sheet IV. Due to unitarity the poles on sheet II, III and IV are situated in the same energy points as the corresponding zeros on sheet I, IV and III, respectively. Note that the size of shift of zeros on sheet IV relative to the ones on sheets I and III is determined by the strength of coupling of the channels (here $\pi\pi$ and $\omega\pi$). The cluster kind is related to the nature of resonance.

With the help of the uniformizing variable[1]

$$v = \frac{(m_\omega + m_{\pi^0})/2 \sqrt{s - 4m_{\pi^+}^2} + m_{\pi^+} \sqrt{s - (m_\omega + m_{\pi^0})^2}}{\sqrt{s\left[((m_\omega + m_{\pi^0})/2)^2 - m_{\pi^+}^2\right]}}, \tag{1}$$

the considered 4-sheeted Riemann surface is mapped onto the v-plane, divided into two parts by a unit circle centered at the origin. Sheets I (II), III (IV) are mapped onto the exterior (interior) of the unit disk on the upper and lower v-half-plane, respectively. The physical region extends from the point i on the imaginary axis ($\pi\pi$ threshold) along the unit circle clockwise in the 1st quadrant to the point 1 on the real axis ($\omega\pi^0$ threshold) and then along the real axis to the point $b = \sqrt{(m_\omega + m_{\pi^0} + 2m_{\pi^+})/(m_\omega + m_{\pi^0} - 2m_{\pi^+})}$ into which $s = \infty$ is mapped on the v-plane. The intervals $(-\infty, -b], [-b^{-1}, b^{-1}], [b, \infty)$ on the real axis are the images of the corresponding edges of the left-hand cut of the $\pi\pi$-scattering amplitude. The (**a**) resonance is represented in $S(\pi\pi \to \pi\pi)$ by two pairs of poles on the images of sheets II and III, symmetric to each other with respect to the imaginary axis, and by zeros, symmetric to these poles with respect to the unit circle. Note that a symmetry of the zeros and poles with respect to the imaginary axis appears due to the real analyticity of the S-matrix, and the symmetry of the poles and zeros with respect to the unit circle ensures a realization of the known experimental fact that the $\pi\pi$ interaction is practically elastic up to a vicinity of the $\omega\pi^0$ threshold.

The resonance part of S-matrix S_{res} becomes *a one-valued function* on the v-plane and, in the $\pi\pi$ channel, it is expressed through the $d(v)$-function as follows[2]:

$$S_{res} = \frac{d(-v^{-1})}{d(v)} \tag{2}$$

where $d(v)$ represents the contribution of resonances, described by one of three types of the pole clusters in the 2-channel case, *i.e.*,

$$d = v^{-M} \prod_{n=1}^{M} (1 - v_n^* v)(1 + v_n v) \tag{3}$$

with M the number of pairs of the conjugate zeros.

The background part S_{bg} is taken in the form:

$$S_{bg} = \exp\left[2i\left(\sqrt{\frac{s - 4m_{\pi^+}^2}{s}}\right)^3 \left(\alpha_1 + \alpha_2 \frac{s - s_1}{s}\theta(s - s_1) + \alpha_3 \frac{s - s_2}{s}\theta(s - s_2)\right)\right] \tag{4}$$

---

[1]The analogous uniformizing variable has been used, *e.g.*, in Ref. [18] in studying the forward elastic $p\bar{p}$ scattering amplitude and in Ref. [19] in the combined analysis of data on processes $\pi\pi \to \pi\pi, K\overline{K}$ in the channel with $I^G J^{PC} = 0^+0^{++}$.

[2]Other authors also have used the parameterizations with the Jost functions at analyzing the S-wave $\pi\pi$ scattering in the one-channel approach [20] and in the two-channel one [21]. In latter work, the uniformizing variable k_2 has been used and the $\pi\pi$-threshold branch-point has been neglected, therefore, their approach cannot be employed near by the $\pi\pi$ threshold.

where $\alpha_i = a_i + ib_i$, s_1 is the threshold of 4π channel noticeable in the ρ-like meson decays, s_2 is the threshold of $\rho 2\pi$ channel. Due to allowing for the left-hand branch-point at $s = 0$ in the uniformizing variable (1), $a_1 = b_1 = 0$. Furthermore, $b_2 = 0$ is an experimental fact.

With formulas (2)–(4), we have analyzed data [14]–[16] for the inelasticity parameter (η) and phase shift of the $\pi\pi$-scattering amplitude (δ) ($S(\pi\pi \to \pi\pi) = \eta \exp(2i\delta)$), introducing three ($\rho(770)$, $\rho(1250 - 1580)$ and $\rho(1550 - 1780)$), four (the indicated ones plus $\rho(1860 - 1910)$) and five (the indicated four plus $\rho(1450)$) resonances. In Ref.[16], results of two analyses are cited: one uses the s-channel helicity amplitude when extracting the $\pi\pi$-scattering amplitude on the π-exchange pole; in the other, the t-channel one is used instead. Therefore, we have taken both analyses as independent. There are given the data for the phase shift of amplitude below the $K\overline{K}$ threshold. Comparing these data with the ones of Refs.[14, 15], one can see that the points of the former lie systematically by 1°-5° higher than the ones of the latter, except for two points of Ref.[14] at 710 and 730 MeV, which lie by about 2° higher than the corresponding points of Ref.[16] and which are omitted in the subsequent analyses. Since we do not know the energy dependence of the remarked deviations of points, we have supposed a constant systematic error that must be determined in the combined analysis of data. We have obtained a satisfactory description with χ^2/NDF and with the indicated systematic error equal respectively to $293.518/(186 - 15) = 1.716$ and $-1.885°$ for the case of three resonances, $280.043/(186 - 19) = 1.677$ and $-1.897°$ for four resonances, $269.574/(186 - 23) = 1.654$ and $-1.876°$ for five resonances. When calculating χ^2 for the inelasticity parameter, three points of data [15] at 990, 1506 and 1825 MeV have been omitted in all three cases as giving the anomalously big contribution to χ^2. When calculating χ^2 for the phase shift, three points of data [16] have been omitted in all three cases: the one at 790 MeV from the s-channel analysis, and two at 790 and 850 MeV from the t-channel one.

On figures 1, we demonstrate results from our fitting to data [14]–[16]. The short-dashed curves are for the three-resonance description, the long-dashed ones for the four-resonance and the solid for the five-resonance cases.

From a variety of possible resonance representations by pole-clusters, the analyses prefer he following one to be the most relevant: *the $\rho(770)$ is described by the cluster of type (**a**) and the others by type (**b**)*.

Let us show the obtained pole clusters on the lower $\sqrt{s}$-half-plane in Table 1 (it is clear there are also complex-conjugate poles on the upper half-plane). The background parameters are: $a_2 = 0.0093$, $a_3 = 0.0618$ and $b_3 = -0.0135$ for the three-resonance, $a_2 = 0.00166$, $a_3 = 0.0433$ and $b_3 = -0.00442$ for the four-resonance and $a_2 = 0.0248$, $a_3 = 0.0841$ and $b_3 = 0.0019$ for the five-resonance descriptions.

Though the description can be considered practically as the same in all three cases, careful consideration of the obtained parameters and energy dependence of the fitted quantities suggests that *the resonance $\rho(1900)$ strongly desired and that the $\rho(1450)$ should be also present improving slightly the description.*

Masses and widths of the obtained ρ-states can be calculated from the pole positions on sheet II for resonances of type (**a**) and on sheet IV for resonances of type (**b**). If the
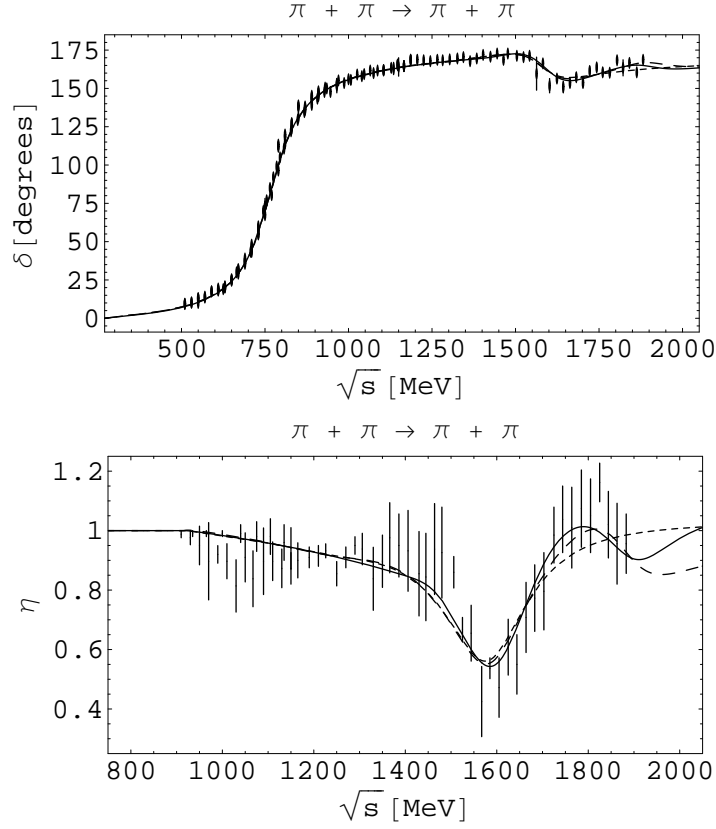
Figure 1: The phase shift of amplitude (the upper figure) and module of matrix element (the lower figure) of the P-wave $\pi\pi$-scattering. The results of 3-resonance (short-dashed), 4-resonance (long-dashed), and 5-resonance (solid) descriptions are shown. The data from Refs. [14]–[16].

resonance part of the amplitude reads as

$$T^{res} = \frac{\sqrt{s}\,\Gamma_{el}}{m_{res}^2 - s - i\sqrt{s}\,\Gamma_{tot}},$$

we obtain for the masses and total widths, respectively, the following values (in the MeV units):

for	$\rho(770)$,	769.3	and	146.6;
for	$\rho(1250)$,	1256.2	and	261.4;
for	$\rho(1470)$,	1468.8	and	200.8;
for	$\rho(1600)$,	1595.1	and	145.8;
for	$\rho(1900)$,	1895.4	and	175.2.

Table 1: Pole clusters for the ρ-like resonances.

Three resonances				
Sheet		II	III	IV
$\rho(770)$	$\sqrt{s_r}$, MeV	$767.3 - i73.3$	$782 - i65.6$	
$\rho(1250)$	$\sqrt{s_r}$, MeV		$1249.9 - i152$	$1249 - i146.2$
$\rho(1600)$	$\sqrt{s_r}$, MeV		$1585 - i130.5$	$1578 - i72.2$
Four resonances				
Sheet		II	III	IV
$\rho(770)$	$\sqrt{s_r}$, MeV	$766.5 - i73.2$	$783.1 - i66.2$	
$\rho(1250)$	$\sqrt{s_r}$, MeV		$1251.4 - i152.1$	$1249 - i144.3$
$\rho(1600)$	$\sqrt{s_r}$, MeV		$1585.2 - i141.8$	$1579.6 - i73.6$
$\rho(1900)$	$\sqrt{s_r}$, MeV		$1871.5 - i97.2$	$1894 - i95.3$
Five resonances				
Sheet		II	III	IV
$\rho(770)$	$\sqrt{s_r}$, MeV	$765.8 - i73.3$	$778.2 - i68.9$	
$\rho(1250)$	$\sqrt{s_r}$, MeV		$1250 - i131.4$	$1249.4 - i130.7$
$\rho(1470)$	$\sqrt{s_r}$, MeV		$1469.2 - i89.3$	$1465.4 - i100.4$
$\rho(1600)$	$\sqrt{s_r}$, MeV		$1634.8 - i145.9$	$1593.4 - i72.9$
$\rho(1900)$	$\sqrt{s_r}$, MeV		$1883 - i106.5$	$1893.4 - i87.6$

3 The Breit–Wigner analysis of P-wave $\pi\pi$ scattering

In various works [1], it was shown that the ρ-like resonances obtained in the previous section have also other considerable decay channels in addition to those considered explicitly above. It was observed that the $\rho(1450)$ and/or a possible $\rho(1250)$ can also decay to the $\eta\rho^0$ ($< 4\%$), $\phi\pi$ ($< 1\%$), and 4π (seen) channels, where the fraction Γ_i/Γ [1] is given in parenthesis. The $\rho(1700)$ resonance has the large branching ratio to the 4π (large), $\rho2\pi$ (dominant) and $\eta\rho^0$ (seen) channels.

To include explicitly influence of some selected channels and to obtain information about couplings with these channels on the basis of analysis of the $\pi\pi$-scattering data, we have used 5-channel Breit–Wigner forms in constructing the Jost matrix determinant $d(k_1, \cdots, k_5)$. To generate the resonance poles and zeros in the S-matrix, the

Le Couteur–Newton relation was utilized:

$$S_{res} = \frac{d(-k_1, \cdots, k_5)}{d(k_1, \cdots, k_5)}. \tag{5}$$

In eq.(5) k_1, k_2, k_3, k_4 and k_5 are the $\pi\pi$-, $\pi^+\pi^-2\pi^0$-, $2(\pi^+\pi^-)$-, $\eta2\pi$- and $\omega\pi^0$-channel momenta, respectively. The d-function is taken as $d = d_{res}d_{bg}$ with d_{res}, describing resonance contributions, and d_{bg}, the background.

The Breit–Wigner form for the resonance part of the d-function is assumed as

$$d_{res}(s) = \prod_r \left[M_r^2 - s - i \sum_{j=1}^{5} \rho_{rj}^3 \, R_{rj} \, f_{rj}^2 \right], \tag{6}$$

where $\rho_{rj} = k_i(s)/k_i(M_r^2)$, f_{rj}^2/M_r is the partial width of resonance with mass M_r, R_{rj} is a Blatt–Weisskopf barrier factor [22] conditioned by the resonance spins. For the vector particle this factor have the form:

$$R_{rj} = \frac{1 + \frac{1}{4}(\sqrt{M_r^2 - 4m_j^2} \, r_{rj})^2}{1 + \frac{1}{4}(\sqrt{s - 4m_j^2} \, r_{rj})^2} \tag{7}$$

with radius $r_{rj} = 0.7035$ fm which in our analysis are equal for all resonances in all channels. Furthermore, we have assumed that the widths of resonance decays to the $\pi^+\pi^-2\pi^0$ and $2(\pi^+\pi^-)$ channels are related by relation: $f_{r2} = f_{r3}/\sqrt{2}$.

The background part d_{bg} is

$$d_{bg} = \exp\left[-i \left(\sqrt{\frac{s - 4m_{\pi^0}^2}{s}} \right)^3 \left(\alpha_1 + \alpha_2 \, \frac{s - s_1}{s} \, \theta(s - s_1) \right) \right] \tag{8}$$

where $\alpha_i = a_i + ib_i$, s_1 is the threshold of $\rho2\pi$ channel (it is clear that a_2 and b_2 take into account also influence of other channels opened at higher energies than the $\rho2\pi$ threshold); b_1 is taken to be zero.

Using formulas (5)–(8) we have performed the analysis, just as in the previous section, with three, four and five resonances. We have obtained the same reasonable description in all three cases: the total $\chi^2/\text{NDF} = 316.206/(186 - 17) = 1.871$, $314.688/(186 - 22) = 1.919$, and $303.101/(186 - 27) = 1.906$ for the case of three, four, and five resonances, respectively. On the figure 2, we demonstrate results of our fitting to data [14]-[16] for the case of five resonances. The systematic error of data [16], discussed in the previous section, is equal to $-1.987°$ in this case. When calculating χ^2 for the inelasticity parameter, three points of data [15] at 990, 1030 and 1825 MeV were omitted as giving the anomalously large contribution to χ^2. When calculating χ^2 for the phase shift, the same three points of data have been omitted as in the model-independent analysis. For the background we find: $a_1 = -0.00121 \pm 0.0018$, $a_2 = -0.1005 \pm 0.011$ and $b_2 = 0.0012 \pm 0.006$.

The obtained values of resonance parameters for the last case are given in Table 2. Note that in Table 2 we do not show the errors for f_{42}, f_{43}, f_{44} and f_{45}, because the
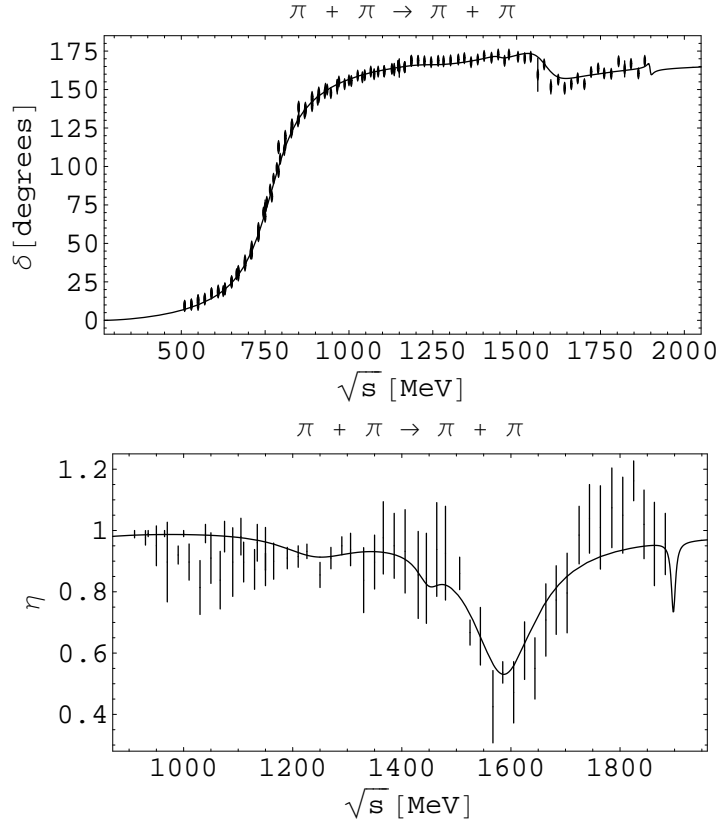
Figure 2: The phase shift of amplitude and module of matrix element of the P-wave $\pi\pi$-scattering. The curves show result of fitting to data [14]–[16] using the Breit-Wigner form.

present data are not sufficient to fix reliably these parameters. We may conclude that, using the accessible data, *the model-independent analysis testifies in favour of existence of the $\rho(1900)$ and, maybe, $\rho(1450)$, but the Breit–Wigner approach cannot verify this result.*

We have also calculated the isovector P-wave length of $\pi\pi$ scattering a_1^1. Its value is shown in Table 3 in comparison with the results from various evaluations in the local [12] and non-local [11] Nambu–Jona-Lasinio (NJL) model and from the ones with the use of Roy's equations [9, 8, 7] (in Ref.[8] one apply also the chiral perturbation theory (ChPT) to construct a precise $\pi\pi$-scattering amplitude at $s^{1/2} \leq 0.8$ GeV).

4   Conclusions

The reasonable description of all the accessible experimental data on the isovector P-wave of $\pi\pi$ scattering for the inelasticity parameter (η) and phase shift of amplitude (δ) [14]-[16] have been obtained up to 1880 MeV based on the first principles (analyticity and unitarity) directly applied to analysis of the data. Analysis has been carried out in

Table 2: The ρ-like resonance parameters (all in MeV).

State	$\rho(770)$	$\rho(1250)$	$\rho(1450)$	$\rho(1600)$	$\rho(1900)$
M	777.69±0.32	1249.8±15.6	1449.9±12.2	1587.3±4.5	1897.8±38
f_{r1}	343.8±0.73	87.7±7.4	56.9±5.4	248.2±5.2	47.3±12
f_{r2}	24.6±5.8	186.3±39.9	100.1±18.7	240.2±8.6	73.7
f_{r3}	34.8±8.2	263.5±56.5	141.6±26.5	339.7±12.5	104.3
f_{r4}		231.8±111	141.2±98	141.8±33	9
f_{r5}		231±115	150±95	108.6±40.4	10
Γ_{tot}	≈154.3	>175	>52	>168	>10

Table 3: Comparison of values of the $\pi\pi$ scattering length a_1^1 from various approaches.

$a_1^1[10^{-3}m_{\pi^+}^{-3}]$	References	Remarks
33.9 ± 2.02	This paper	Breit–Wigner analysis
34	[12]	Local NJL model
37	[11]	Non-local NJL model
37.9 ± 0.5	[8]	Roy equations using ChPT
38.4 ± 0.8	[9]	Roy equations
39.6 ± 2.4	[7]	Roy equations

the model-independent approach using the uniformizing variable (here the satisfactory description is obtained: $\chi^2/\text{NDF} = 1.654$) and applying multichannel Breit–Wigner forms to generate the resonance poles and zeros in the S-matrix ($\chi^2/\text{NDF} = 1.906$). The aim of analysis (except for obtaining an unified formula for the P-wave $\pi\pi$ scattering amplitude in the whole of investigated energy range) was to study the ρ-like mesons below 1900 MeV and to obtain the P-wave $\pi\pi$-scattering length.

For the $\rho(770)$, the obtained value for mass is a little smaller in the model-independent approach (769.3 MeV) and a little bigger in the Breit–Wigner one (777.69 ± 0.32 MeV) than the averaged mass (775.5 ± 0.4 MeV) cited in the PDG tables [1]. However, this mass also occurs in analysis of some reactions [1]. The obtained value of the total width in the first analysis (146.6 MeV) coincides with the averaged PDG one (146.4±1.1 MeV) and it is a little bit bigger in the second analysis ($\approx$ 154.3 MeV) than the PDG value, however, this is also encountered in other analyses [1]. Note that predicted widths of the $\rho(770)$ decays to the 4π-modes are significantly larger than, *e.g.*, those evaluated in the chiral model of some mesons based on the hidden local symmetry added with the

anomalous terms [23].

The 2nd ρ-like meson has the mass 1256.2 MeV in the 1st analysis and 1249.8±15.6 MeV in the 2nd one. This differs significantly from the mass (1459±11 MeV) of the 2nd ρ-like meson cited in the PDG tables [1]. We mentioned already in Introduction that the ρ(1250) meson was discussed actively some time ago [2, 3], and next the evidence for it was obtained in some analyses [4, 5]. Note also the talk by Ichiro Yamauchi at the HADRON'07 conference [24] in which this mass value of the second ρ-like meson is also confirmed in the re-analysis of some data on the $e^+e^- \to \omega\pi^0$ reaction. To the point, if this state is interpreted as a first radial excitation of the 1^+1^{--} state, then it lies down well on the corresponding linear trajectory with an universal slope on the (n, M^2) plane [25] (n is the radial quantum number of the $q\bar{q}$ state), while the meson with mass $M = 1450$ MeV turns out to be considerably higher than this trajectory.

Further we note that some time ago it was shown that the 1600-MeV region contains in fact two ρ-like mesons. This conclusion was made on the basis of investigation of the consistency of the 2π and 4π electromagnetic form factors and the $\pi\pi$-scattering length [26] and as a result of combined analysis of data on the 2π and 4π final states in e^+e^- annihilation and photoproduction [27]. We assume this possibility, *i.e.*, that *in the energy range 1200–1800 MeV there are three ρ-like mesons and the next meson has the mass about 1450 MeV.* This does not contradict to data; in the model-independent analysis, description is even slightly better than without this state. It seems that this improvement of description can become more remarkable at an explicit consideration of the $\eta 2\pi$-threshold in the uniformizing variable, because the Breit–Wigner analysis points to the considerable coupling of the ρ-like mesons with the $\eta 2\pi$ channel. However for the final conclusion the combined analysis of several processes to which the investigated resonances are appreciably coupled have to be performed.

The fourth ρ-like meson turns out to have the mass about 1600 MeV rather than 1720 MeV cited in the PDG tables [1]. Note that in a number of previous analyses of some reactions one has also obtained the resonance with mass near 1600 MeV [1]. Note also a rather big obtained coupling of these ρ-like mesons with the 4π channels.

As to the ρ(1900), in this region there are practically no data on the P-wave of $\pi\pi$ scattering. The model-independent analysis, maybe, somehow testifies in favour of existence of this state, whereas the Breit–Wigner one gives the same description with and without the ρ(1900). For more definite conclusion about this state, the P-wave $\pi\pi$ scattering data above 1880 MeV are needed. Furthermore, the combined analysis of coupled processes should be carried out.

Finally, we note that the P-wave $\pi\pi$ scattering length ($a_1^1 = 33.9 \pm 2.02$ $[10^{-3}m_{\pi^+}^{-3}]$), obtained in the Breit–Wigner analysis, matches most to the one in the local Nambu–Jona-Lasinio model [12].

5   Acknowledgements

References

[1] W.-M. Yao *et al.* (PDG), J. Phys. G **33**, 1 (2006).

[2] N.M. Budnev, V.M. Budnev and V.V. Serebryakov, Phys. Lett. B **70**, 365 (1977).

[3] S.B. Gerasimov and A.B. Govorkov, Z. Phys. C **13**, 43 (1982).

[4] D. Aston *et al.*, Nucl. Phys. B (Proc. Suppl.) **21**, 105 (1991).

[5] T.S. Belozerova and V.K. Henner, Phys. Elem. Part. At. Nucl. **29**, part 1, 148 (1998).

[6] I. Caprini *et al.*, Phys.Rev. D **68**, 074006 (2003).

[7] R. Kamiński, L. Leśniak, and B. Loiseau, Phys. Lett. B**551**, 241 (2003).

[8] I. Caprini, G. Colangelo and H. Leutwyler, Int. J. Mod. Phys. A **21**, 954 (2006).

[9] J.R. Peláez and F.J. Ynduráin, Phys. Rev. D **71**, 074016 (2005).

[10] R. Kaminski, J.R. Pelaez and F.J. Yndurain, Phys.Rev. D **74**, 014001 (2006); Erratum-ibid. D **74**, 079903 (2006).

[11] A.A. Osipov, A.E. Radzhabov and M.K. Volkov, hep-ph/0603130.

[12] V. Bernard, A.A. Osipov and U.G. Meissner, Phys. Lett. B **285**, 119 (1992).

[13] D. Krupa, V.A. Meshcheryakov, Yu.S. Surovtsev, Nuovo Cimento A **109**, 281 (1996).

[14] S.D. Protopopescu *et al.*, Phys. Rev. D **7**, 1279 (1973).

[15] B. Hyams *et al.*, Nucl. Phys. B **64**, 134 (1973).

[16] P. Estabrooks and A.D. Martin, Nucl. Phys. B **79**, 301 (1974).

[17] K.J. Le Couteur, Proc. Roy. Soc. A **256**, 115 (1960); R.G. Newton, J. Math. Phys. **2**, 188 (1961).

[18] B.V. Bykovsky, V.A. Meshcheryakov and D.V. Meshcheryakov, Yad. Fiz. **53**, 257 (1990).

[19] Yu.S. Surovtsev, D. Krupa and M. Nagy, Eur. Phys. J. A **15**, 409 (2002).

[20] J. Bohacik and H. Kühnelt, Phys. Rev. D **21**, 1342 (1980).

[21] D. Morgan and M.R. Pennington, Phys. Rev. D **48**, 1185 (1993).

[22] J. Blatt and V. Weisskopf, *Theoretical nuclear physics*, Wiley, N.Y., 1952.

[23] N.N. Achasov and A.A. Kozhevnikov, Phys. Rev. D **71**, 034015 (2005).

[24] I.Yamauchi and T. Komada, *Further properties of extra light-vector mesons omega′(1300) and rho′(1300)*, Talk at the XII Int. Conf. on Hadron Spectroscopy - Hadron07 (8-13 October 2007, Frascati, Italy), to be published in Frascati Physics Series, Volume XLVI (2007).

[25] A.V. Anisovich, V.V. Anisovich and A.V. Sarantsev, Phys. Rev. D **62**, 051502 (2000).

[26] C. Erkal and M.G. Olsson, Z. Phys. C **31**, 615 (1986).

[27] A. Donnachie and H. Mirzaie, Z. Phys. C **33**, 407 (1987).